**Supplementary information for:**

# Activatable zymography probes enable in situ localization of protease dysregulation in cancer

**Authors:** Ava P. Soleimany[1,2,3†], Jesse D. Kirkpatrick[1,2†], Susan Su[1,4], Jaideep S. Dudani[1,5], Qian Zhong[1], Ahmet Bekdemir[1,2], Sangeeta N. Bhatia[1,2,6-10*]

**Affiliations:**

[1]Koch Institute for Integrative Cancer Research, Massachusetts Institute of Technology, Cambridge, MA 02139.

[2]Harvard-MIT Division of Health Sciences and Technology, Institute for Medical Engineering and Science, Massachusetts Institute of Technology, Cambridge, MA 02139.

[3]Harvard Graduate Program in Biophysics, Harvard University, Boston, MA 02115.

[4]Department of Mechanical Engineering, Massachusetts Institute of Technology, Cambridge, MA 02139.

[5]Department of Biological Engineering, Massachusetts Institute of Technology, Cambridge, MA 02139.

[6]Howard Hughes Medical Institute, Cambridge, MA 02139.

[7]Department of Electrical Engineering and Computer Science, Massachusetts Institute of Technology, Cambridge, MA 02139.

[8]Department of Medicine, Brigham and Women's Hospital, Harvard Medical School, Boston, MA 02115.

[9]Broad Institute of Massachusetts Institute of Technology and Harvard, Cambridge, MA 02139.

[10]Wyss Institute at Harvard, Boston, MA 02115.

[†]These authors contributed equally to this work.

*Corresponding author. Email: sbhatia@mit.edu

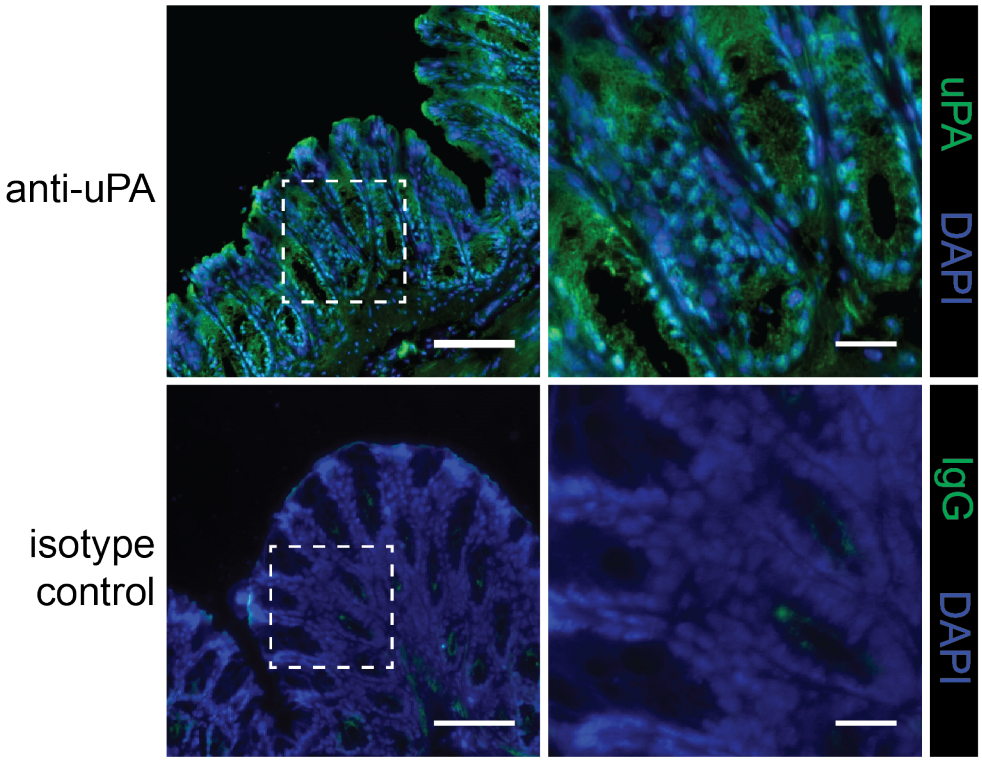


**Supplementary Figure S1. uPA abundance in colon tissue sections.** Immunofluorescence staining for uPA (top, green) in fresh-frozen sections of healthy mouse colon. A consecutive section was stained with an IgG isotype control (bottom, green). Images on right show higher magnification view of boxed regions. Scale bars, left = 100 µm; scale bars, right = 25 µm.

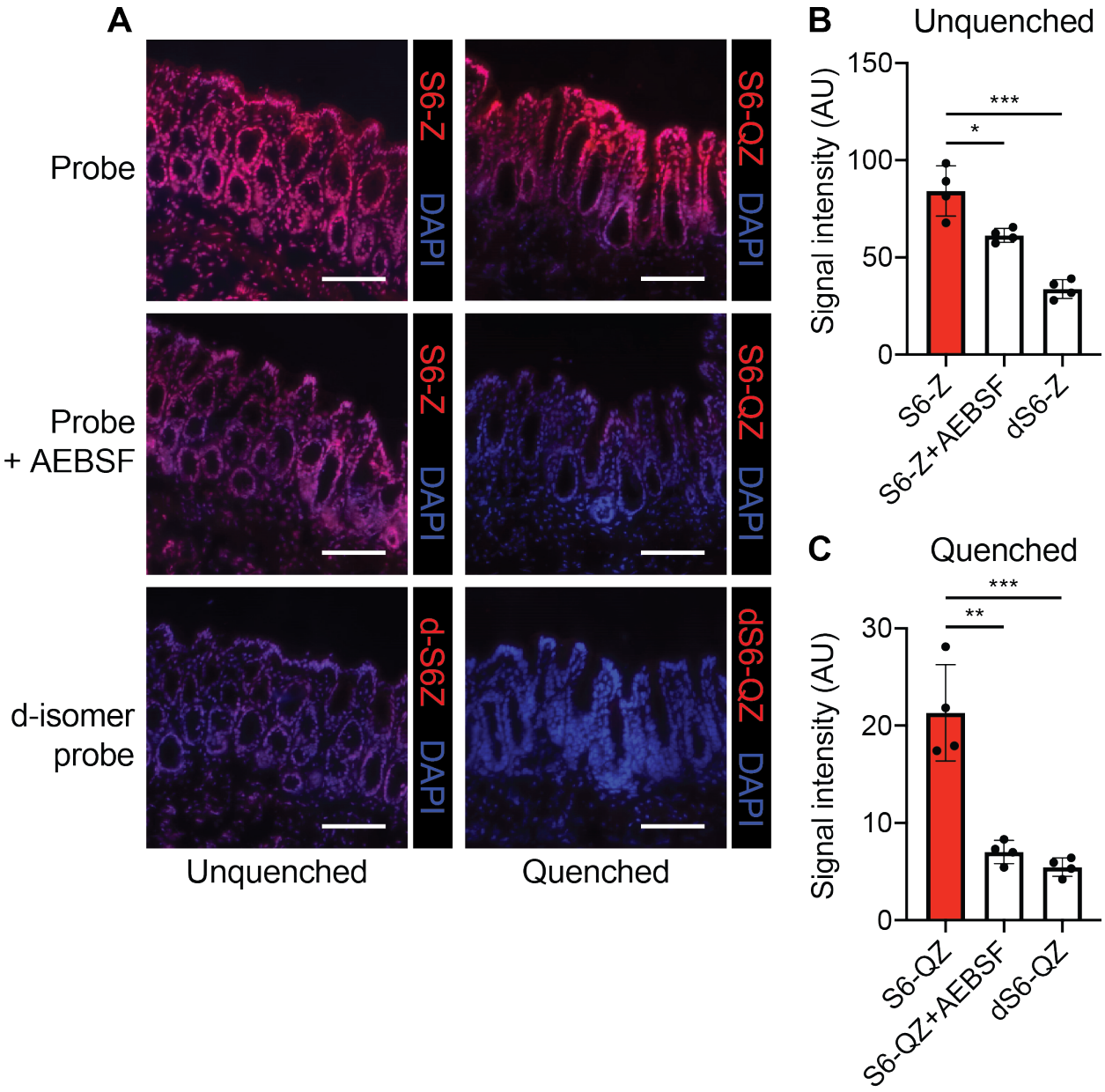


**Supplementary Figure S2. Comparison of unquenched and quenched AZPs. A,** Serine protease-cleavable unquenched and quenched AZPs, S6-Z and S6-QZ, respectively, were applied to fresh-frozen sections of healthy mouse colon. Staining of frozen colon sections with cleavable probes (S6-Z, S6-QZ; top, red), cleavable probes with the serine protease inhibitor AEBSF (middle, red), or the uncleavable *d*-stereoisomer probe (dS6-Z, dS6-QZ; bottom, red). All sections were counterstained with DAPI (blue). Different brightness settings were used for imaging staining of unquenched and quenched probes to enable visualization of differences in background probe binding. **B,** Fraction of detected nuclei positive for S6-Z or dS6-Z in epithelial regions of colon tissue sections ($n$ = 4 consecutive sections per group; mean ± s.d.; two-tailed unpaired $t$-test, *$P$ = 0.0145, ***$P$ = 0.000340). **C,** Fraction of detected nuclei positive for S6-QZ or dS6-QZ in epithelial regions of colon tissue sections ($n$ = 4 consecutive sections per group; mean ± s.d.; two-tailed unpaired $t$-test, **$P$ = 0.00135, ***$P$ = 0.000748). All scale bars = 100 µm.

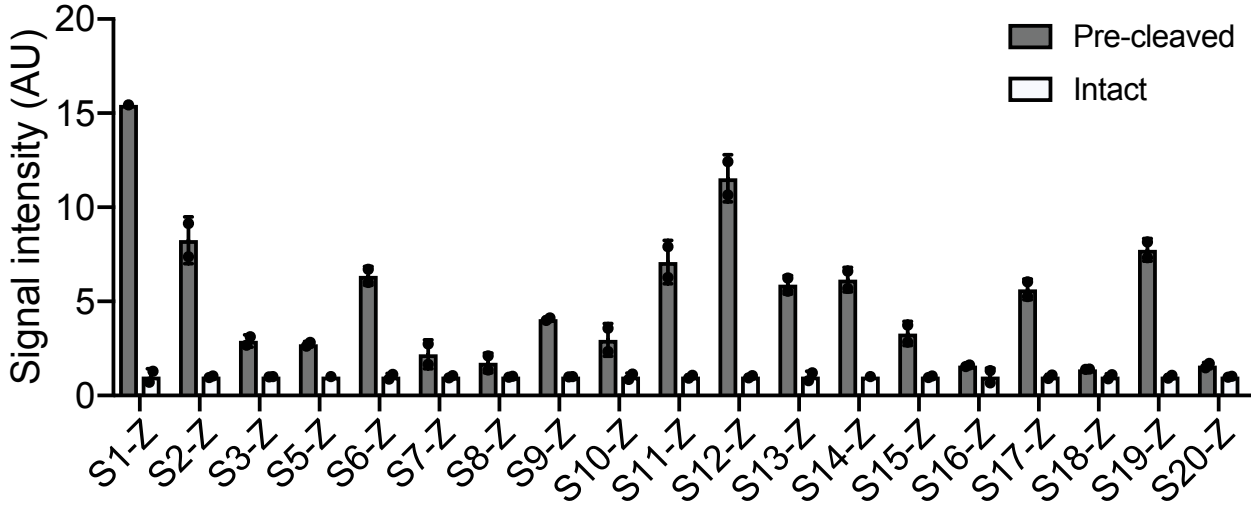


**Supplementary Figure S3. AZP library characterization.** AZPs, either intact or with linkers pre-cleaved by a cognate recombinant protease, were applied to fresh-frozen colon tissue for 30 minutes, and fluorescent signal intensity of bound probes was quantified (*n* = 1-2 replicates per probe; mean ± s.d.).

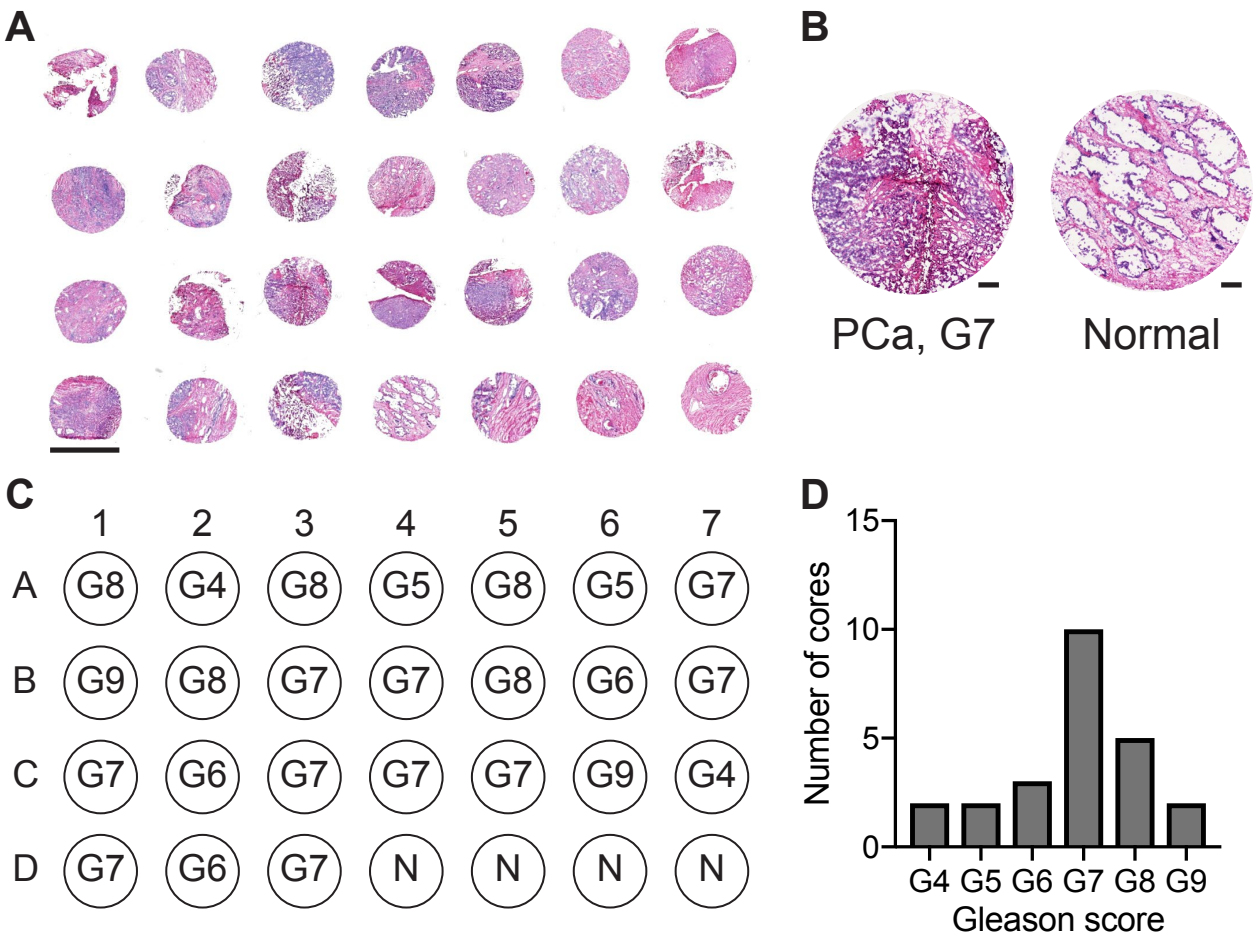


**Supplementary Figure S4. Fresh-frozen human prostate cancer tissue microarray (TMA).** **A,** H&E stain of human prostate cancer (PCa) TMA. Scale bar = 2 mm. **B,** Hematoxylin and eosin stain of select biopsy cores from Gleason 7 PCa tumor (left) and normal prostate (right). Scale bars = 200 μm. **C,** TMA map detailing the Gleason scores (i.e., G4-G10) for prostate cancer specimens. N = normal. **D,** Distribution across Gleason scores for cores in the TMA.

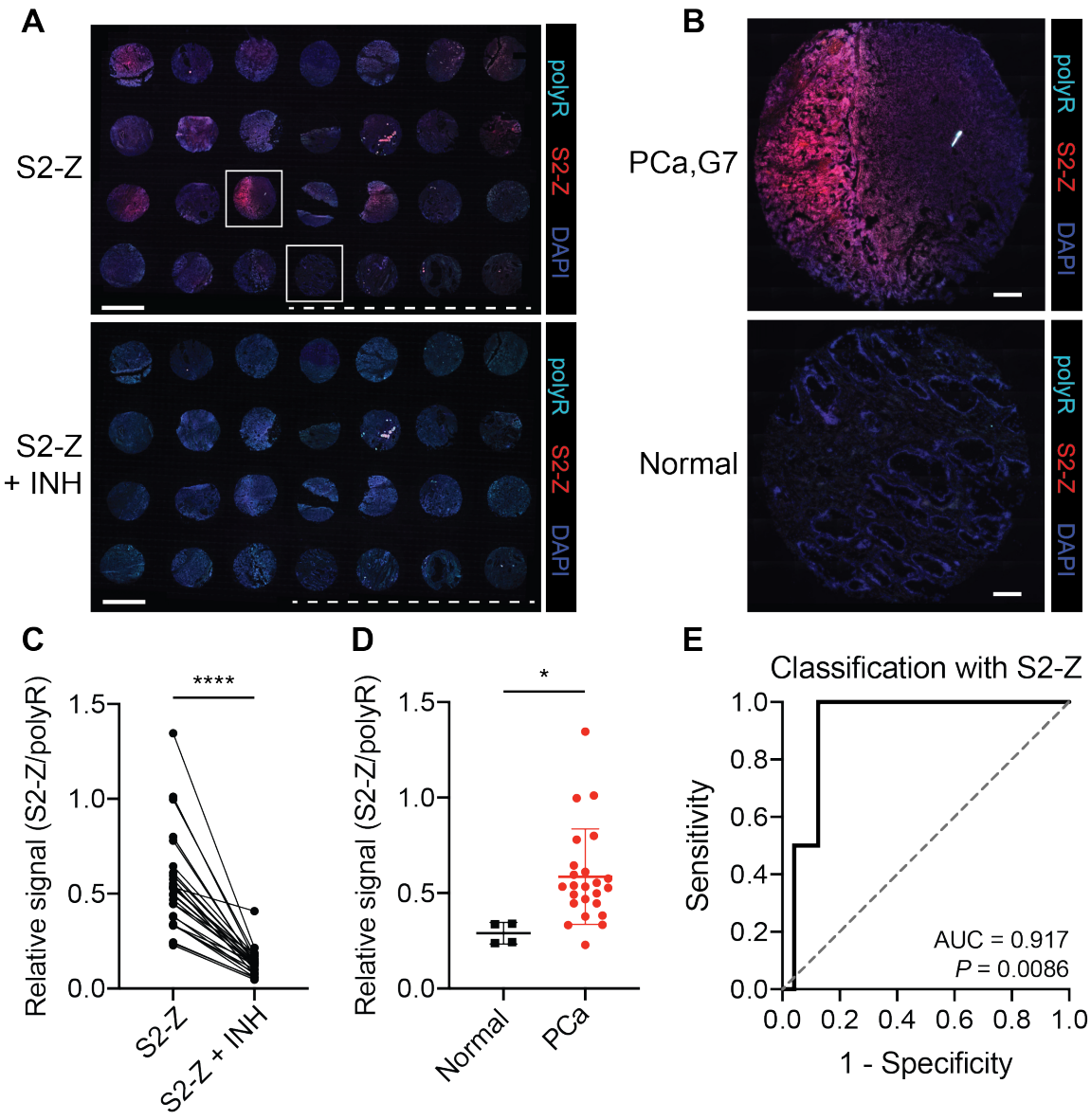


**Supplementary Figure S5. S2-Z selectively labels human PCa tissue. A,** Application of S2-Z AZP (red) to a human PCa tissue microarray (TMA) consisting of 24 prostate adenocarcinoma samples and 4 normal prostate samples (S2-Z, top). A consecutive TMA was stained with S2-Z along with a cocktail of protease inhibitors (S2-Z + INH, bottom). Sections were stained with a polyR binding control (teal) and counterstained with DAPI (blue). Dotted lines are shown below normal prostate samples. Scale bars = 2 mm. **B,** Higher-magnification image of boxed cores from (A) showing Gleason 7 PCa (top) and normal prostate (bottom). Scale bars = 200 µm. **C,** Quantification of average S2-Z intensity relative to polyR (binding control) intensity across each TMA core ($n$ = 28) for sections incubated with (S2-Z + INH) and without (S2-Z) protease inhibitors (two-tailed paired $t$-test, ****$P$ < 0.0001). **D,** Quantification of relative S2-Z intensity from normal ($n$ = 4) and PCa tumor ($n$ = 24) cores (mean ± s.d.; two-tailed unpaired $t$-test, *$P$ = 0.0284). **E,** Receiver-operating characteristic (ROC) curve showing performance of relative AZP signal (S2-Z/polyR) in discriminating normal from PCa tumor cores (AUC = 0.917, 95% confidence interval 0.8103-1.000; $P$ = 0.0086 from random classifier shown in dashed line).

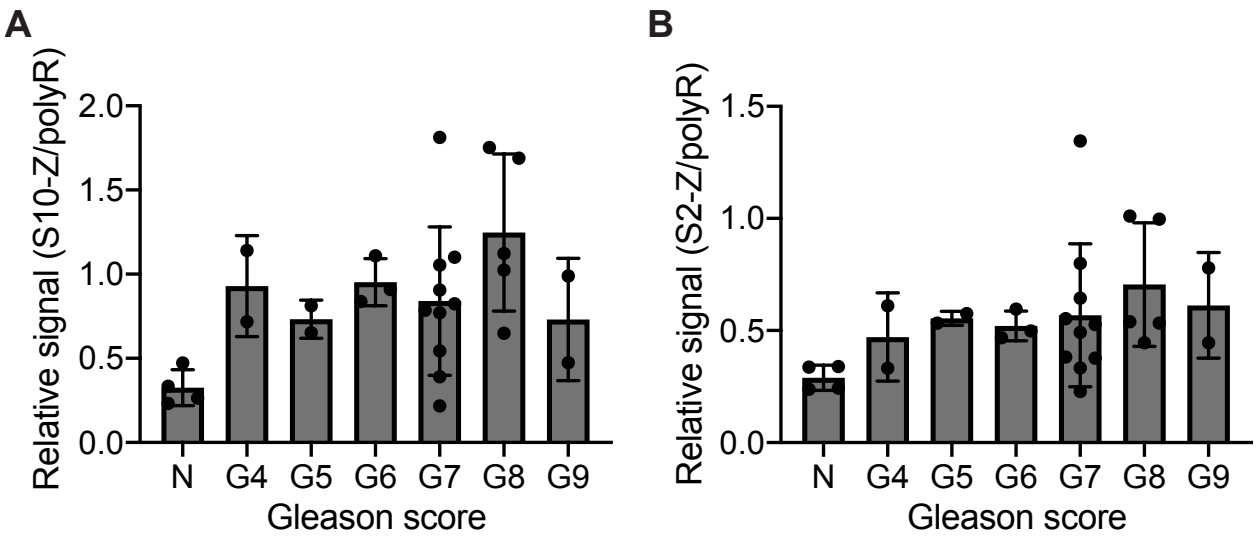


**Supplementary Figure S6. Distribution of AZP staining intensities in human PCa TMA.** Distribution of relative S10-Z (**A**) and S2-Z (**B**) intensities across Gleason scores across the TMA (N = normal; AZP intensities normalized to polyR binding control).

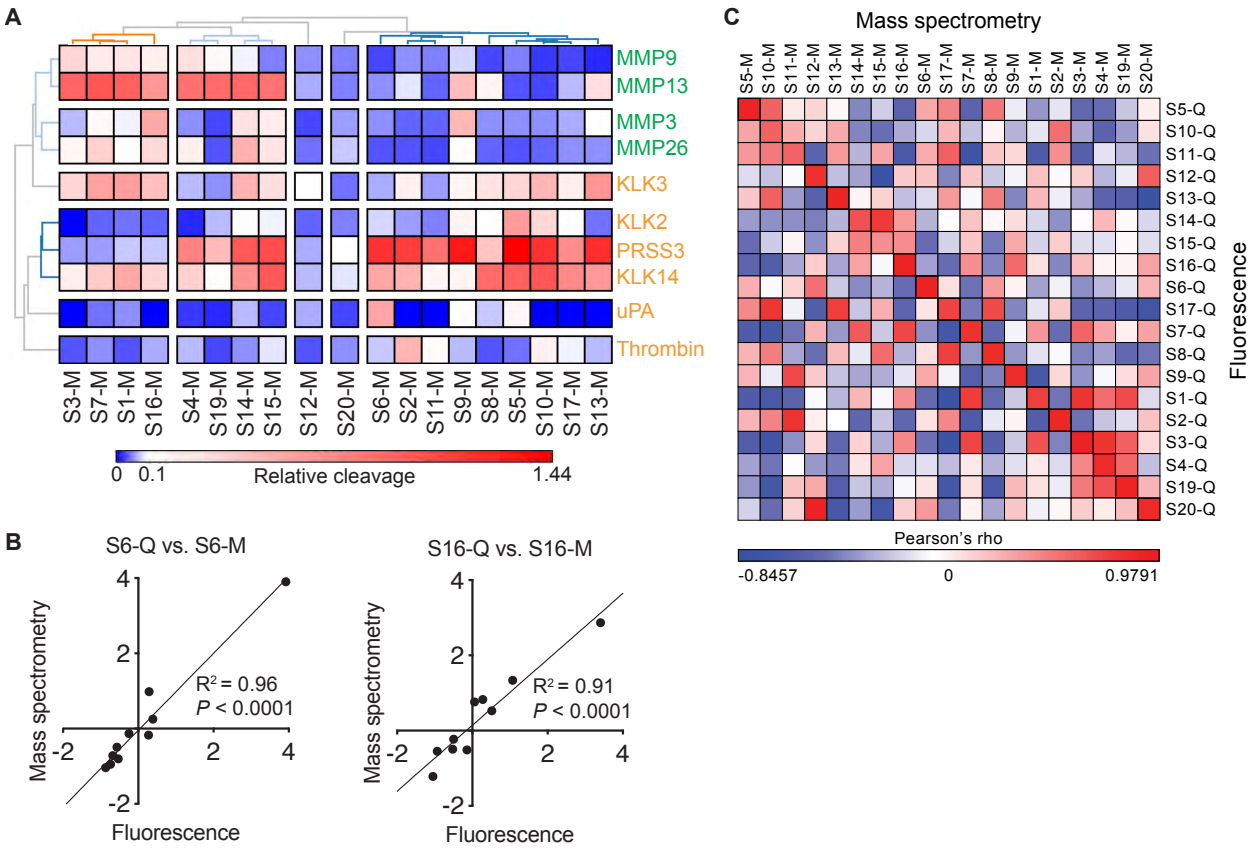


**Supplementary Figure S7. Protease activity profiling with barcoded substrate libraries. A,** Heat map showing *in vitro* cleavage of mass-barcoded substrates (x-axis) by selected recombinant proteases (y-axis; metalloproteinases, green; serine proteases, yellow). Cleavage products were quantified by mass spectrometry, and unsupervised hierarchical clustering was performed (*n* = 2 replicates per protease). **B,** Comparison of relative substrate cleavage *z*-scores for serine protease substrate S6-Q/S6-M (quenched/mass encoded, respectively) and metalloproteinase substrate S16-Q/S16-M (quenched/mass encoded, respectively), as measured by fluorescence with quenched substrates (x-axis) and mass spectrometry with bead-conjugated substrates (y-axis) (linear regression; S6 $R^2$ = 0.96, $P$ < 0.0001 from non-zero slope; S16 $R^2$ = 0.91, $P$ < 0.0001 from non-zero slope)**. C,** Correlation of cleavage *z*-scores of FRET-paired free peptides to cleavage *z*-scores of mass-barcoded peptides conjugated to the surface of magnetic beads, calculated as Pearson's rho across all proteases using cleavage *z*-scores.

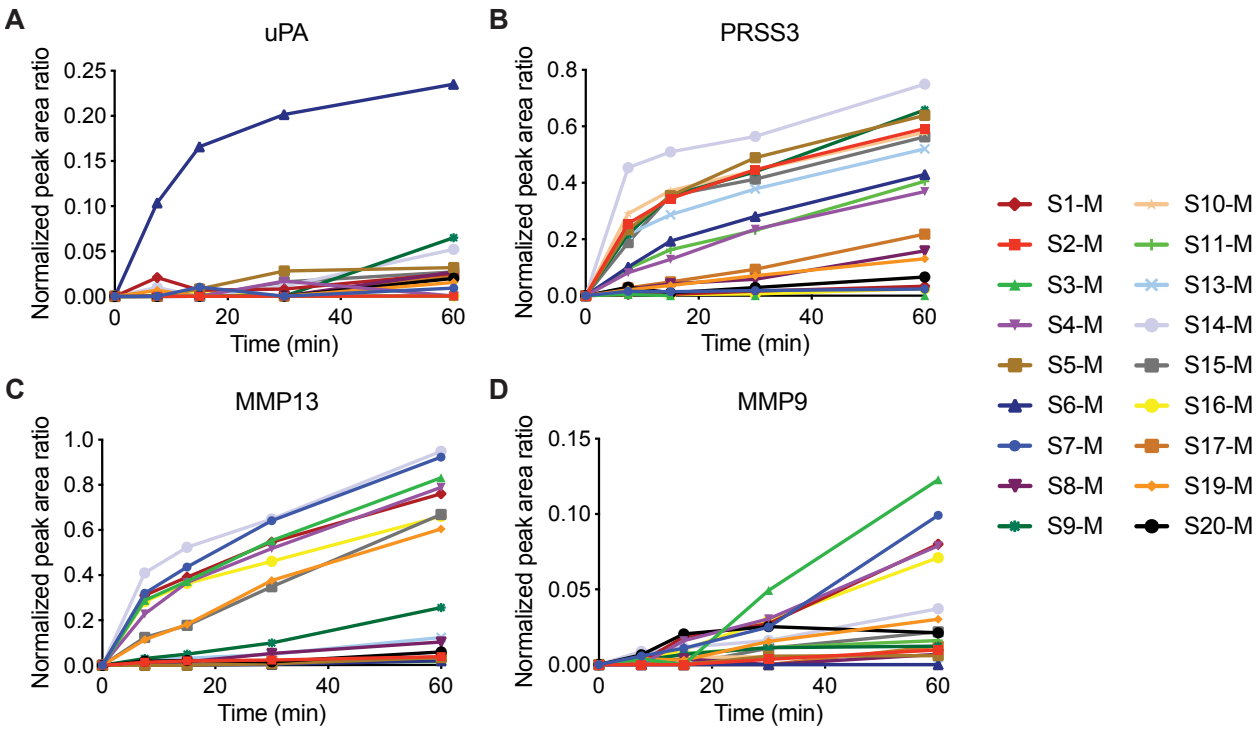


**Supplementary Figure S8. Profiling cleavage kinetics using mass-barcoded bead library.** Kinetics of substrate cleavage obtained from mass-barcoded library screen for the serine proteases uPA (**A**) and PRSS3 (**B**) and the metalloproteinases MMP13 (**C**) and MMP9 (**D**). Kinetics were assessed via quantification of liberated barcodes isolated via magnetic separation at various time points after addition of protease, followed by mass spectrometry quantification with LC-MS/MS. Lines represent means of two independent measurements.

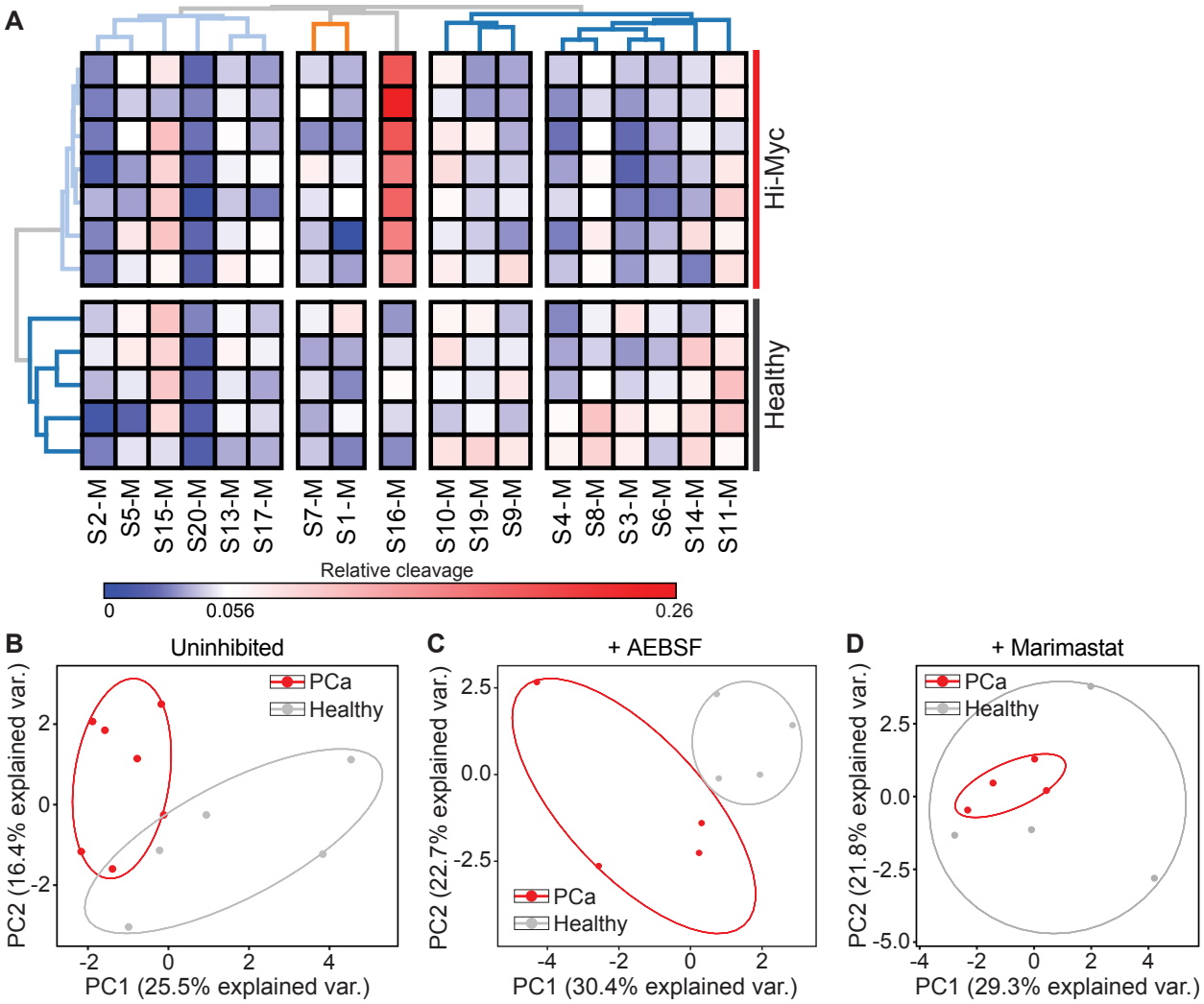


**Supplementary Figure S9. Differential cleavage of peptide S16 is driven by MMP dysregulation and drives differentiation of Hi-Myc from healthy prostates. A,** Hierarchical clustering of cleavage data from multiplexed protease substrate screen of mass-encoded bead library against homogenates of prostates from healthy (gray, *n* = 5) and Hi-Myc (red, *n* = 7) mice. **B-D,** Principal component analysis (PCA) of cleavage data from homogenates incubated without inhibitor (B), with the serine protease inhibitor AEBSF (C), or with the metalloproteinase inhibitor marimastat (D).

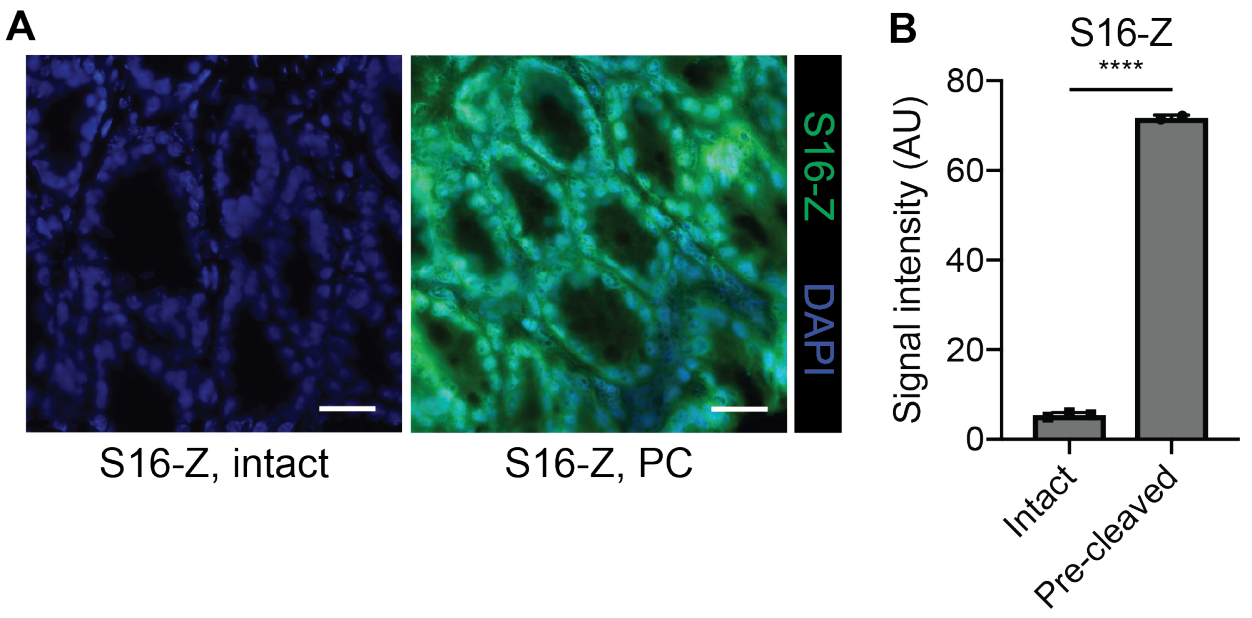


**Supplementary Figure S10. S16-Z tissue binding depends on proteolytic cleavage. A,** Binding of intact or MMP12 pre-cleaved (PC) S16-Z (green) to fresh-frozen mouse colon tissue following incubation at 4° C. Sections were counterstained with DAPI (blue). Scale bars = 25 µm. **B,** Quantification of S16-Z binding for intact probe or probe pre-cleaved by MMP12 (*n* = 2-3 replicates; mean ± s.d.; two-tailed unpaired *t*-test, ****$P < 0.0001$).

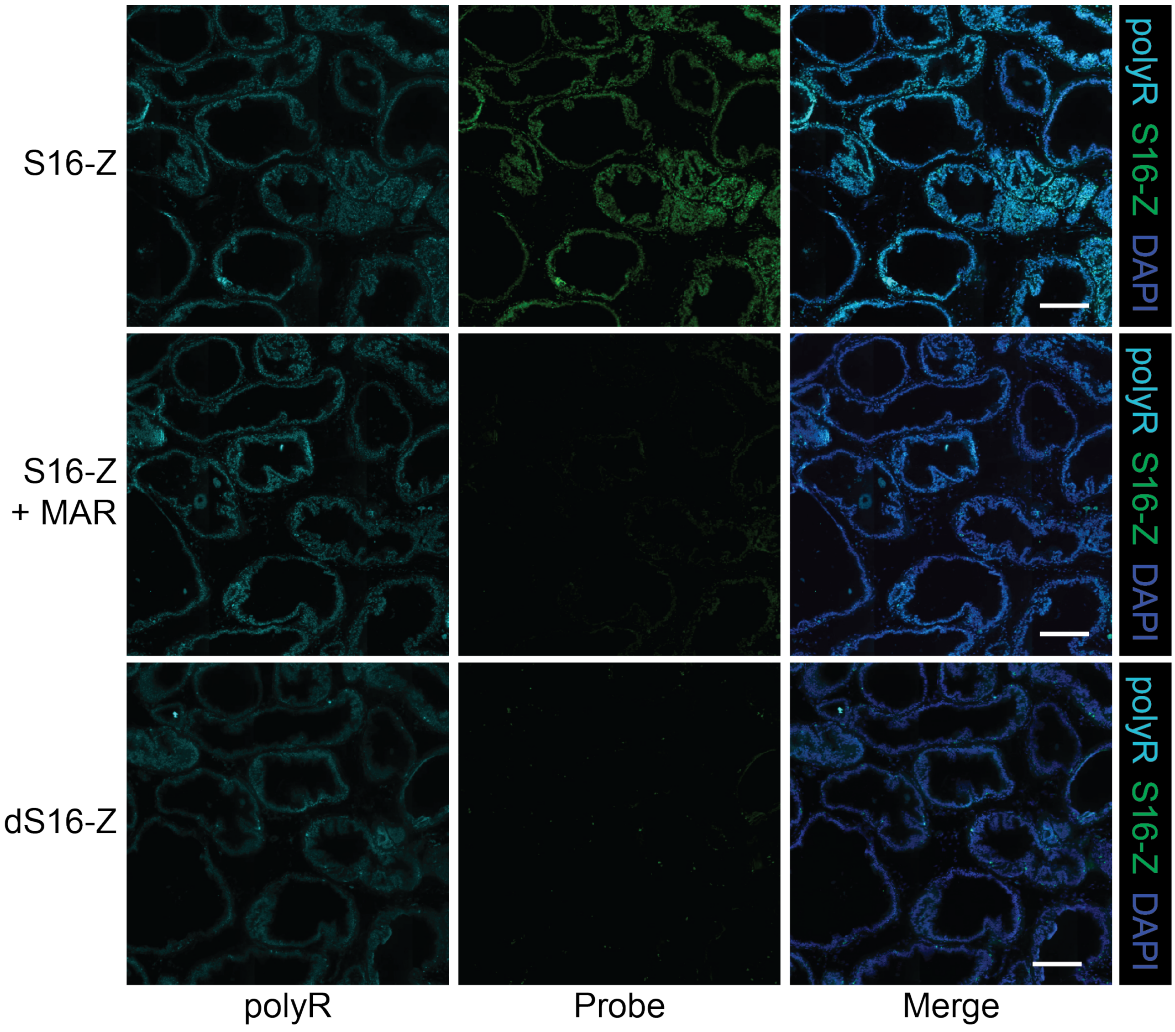


**Supplementary Figure S11. S16-Z labeling of Hi-Myc tissue is dependent on *in situ* MMP activity.** Staining of Hi-Myc tissue with polyR (left column, teal) and either MMP-activatable S16-Z (top and middle rows; green) or *d*-stereoisomer dS16-Z (bottom row; green). Top and middle rows show staining of consecutive sections without (top) and with (middle) the MMP inhibitor marimastat (MAR). Sections were counterstained with DAPI (blue). Scale bars = 200 μm.

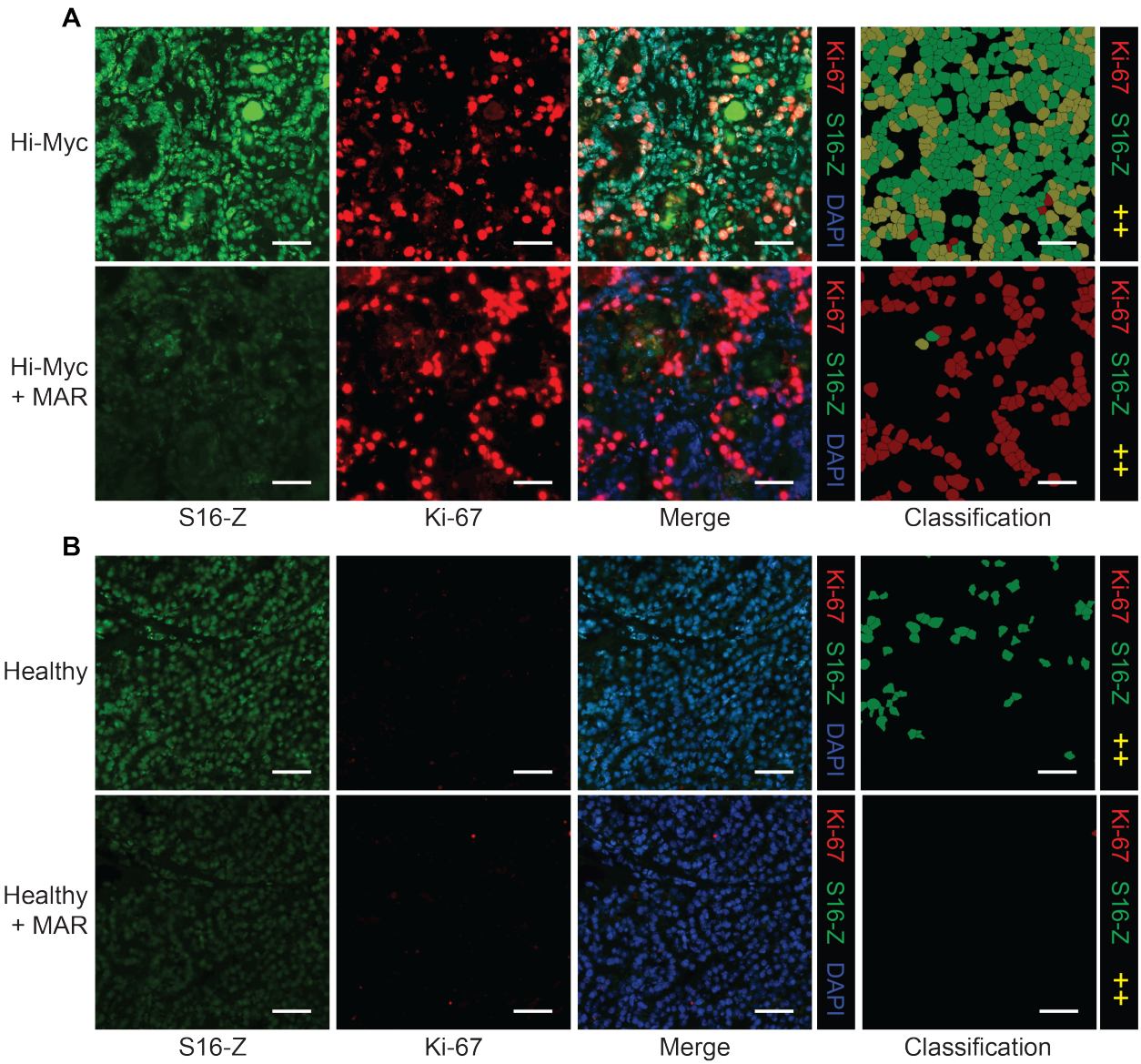


**Supplementary Figure S12. MMP activity drives S16-Z labeling of proliferative tumor regions in Hi-Myc prostates. A, B,** Staining of Hi-Myc tumor region (A) and healthy prostate tissue (B) with S16-Z (green) with co-staining for the proliferation marker Ki-67 (red). Consecutive sections were stained with S16-Z and Ki-67 in the presence of marimastat (MAR). Sections were counterstained with DAPI (blue). Detected cells were classified on the basis of S16-Z and Ki-67 staining intensities to produce cellular classification maps (green: S16-Z+, red: Ki-67+, yellow: S16-Z+ and Ki-67+). Scale bars = 50 µm.

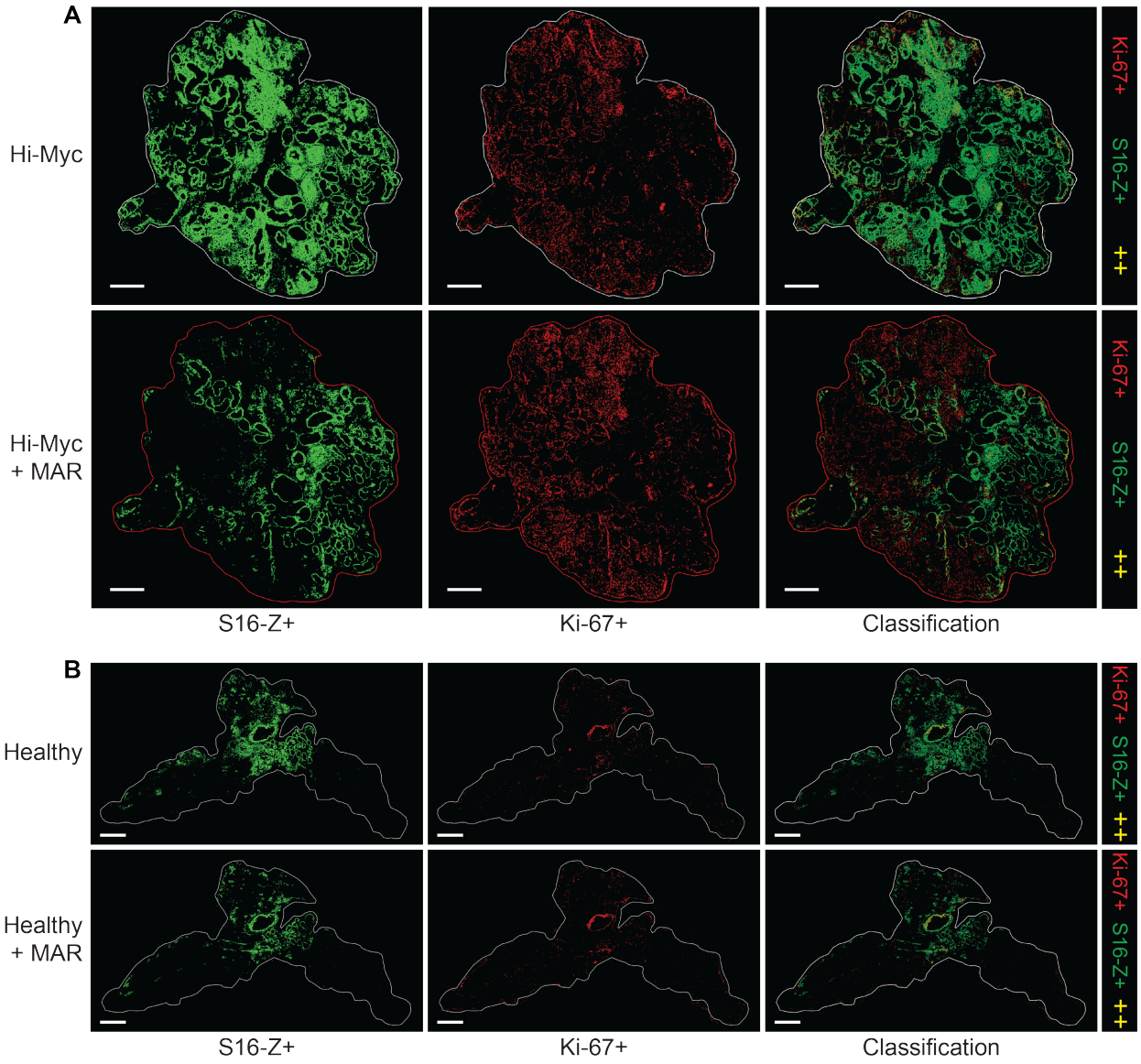


**Supplementary Figure S13. S16-Z and Ki-67 staining of healthy and Hi-Myc prostate whole tissue sections. A, B,** S16-Z, with or without MAR, was applied to prostate tissues from Hi-Myc (A) and healthy (B) mice with co-staining for the proliferation marker Ki-67. Detected cells were classified on the basis of S16-Z and Ki-67 staining intensities to produce classification maps of whole tissue sections (green: S16-Z+, red: Ki-67+, yellow: S16-Z+ and Ki-67+). Scale bars = 1 mm.

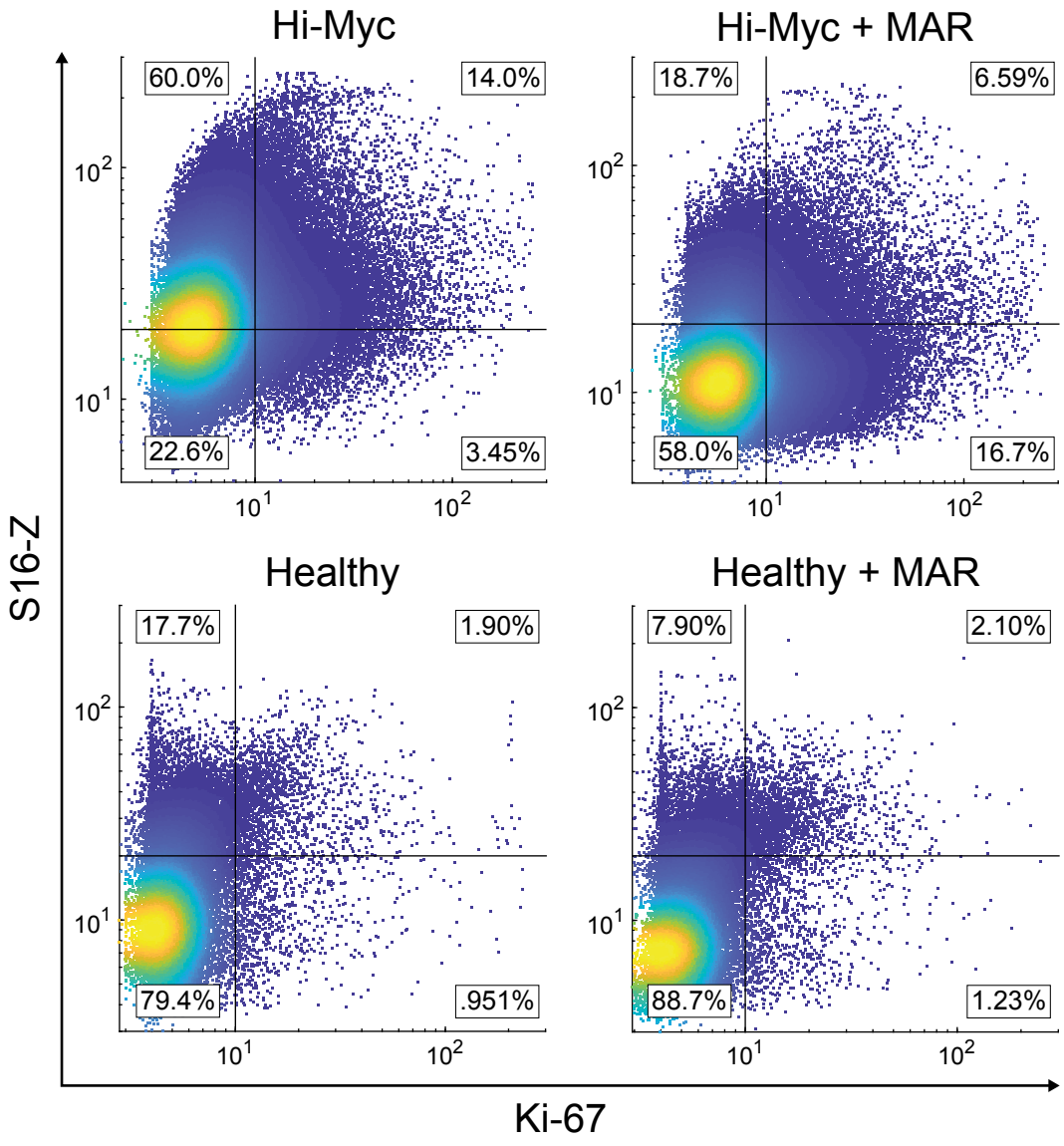


**Supplementary Figure S14. Whole sample, cell-by-cell quantification of S16-Z and Ki-67 fluorescent staining.** Cell-by-cell quantification of S16-Z and Ki-67 fluorescence intensity in detected nuclei from representative Hi-Myc and healthy prostate tissue sections incubated with or without the MMP inhibitor marimastat (MAR). Lines represent thresholds for positivity for each of the markers.

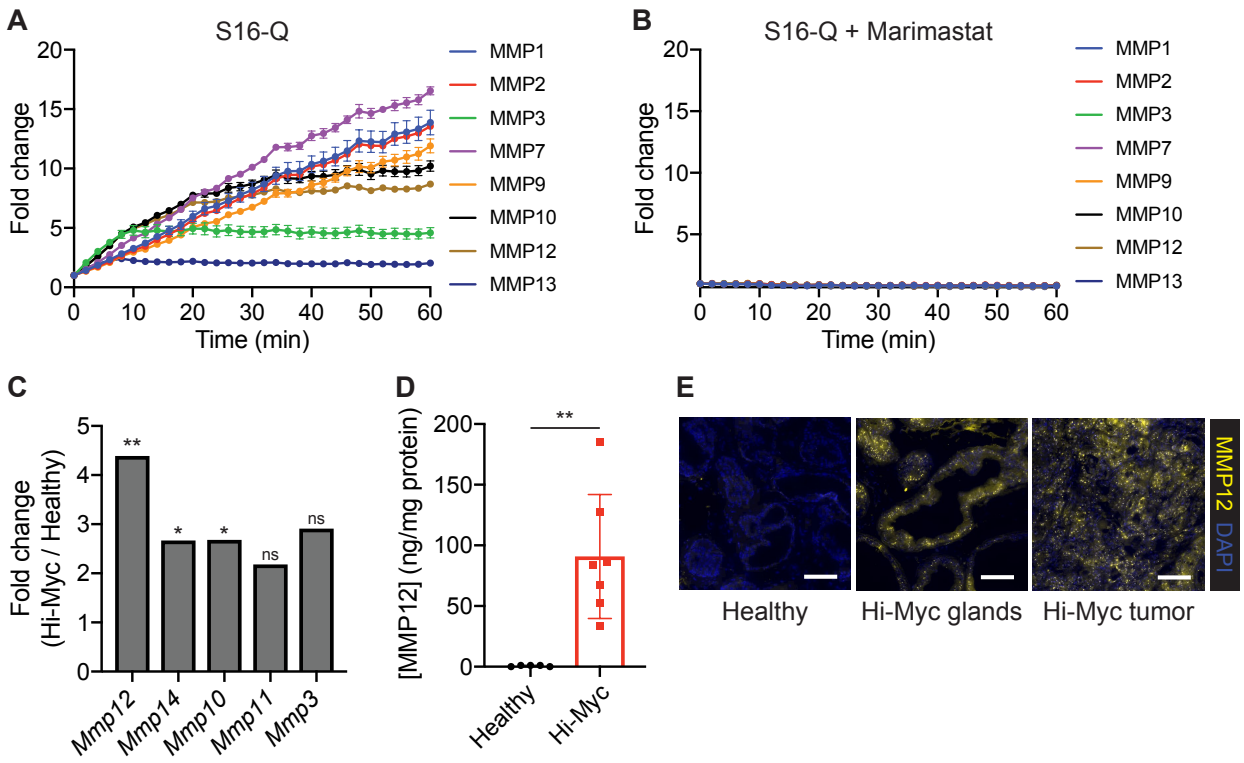


**Supplementary Figure S15. Characterization of MMP12 dysregulation in the Hi-Myc model.** **A,** Fluorescent dequenching measurements for panel of MMPs against fluorescent version (S16-Q) of Hi-Myc-responsive substrate S16 (*n* = 2 replicates per protease; mean ± s.d.). **B,** Addition of MMP inhibitor marimastat (MAR) abrogated fluorescence increase for panel of MMPs against S16-Q (*n* = 2 replicates per protease; mean ± s.d.). **C,** Relative expression of the top 5 MMPs most significantly upregulated in Hi-Myc prostates relative to age-matched healthy controls, analyzed by Affymetrix microarray, adapted from Ellwood-Yen et al., *Cancer Cell* 2003[1] (two-tailed unpaired *t*-test; ***P* < 0.01, **P* < 0.05, ns = not significant). **D,** Enzyme-linked immunosorbent assay (ELISA) results comparing protein-level abundance of MMP12 in homogenates of Hi-Myc prostates relative to age-matched healthy controls (*n* = 7 Hi-Myc, *n* = 5 healthy; mean ± s.d.; Welch's unequal variances *t*-test; ***P* = 0.0034). **E,** Immunofluorescence staining for MMP12 (yellow) in fresh-frozen sections of healthy and Hi-Myc prostates, showing histologically similar regions of healthy and Hi-Myc prostates (Healthy, Hi-Myc glands) as well as a Hi-Myc tumor region (Hi-Myc tumor). Scale bars = 100 μm.

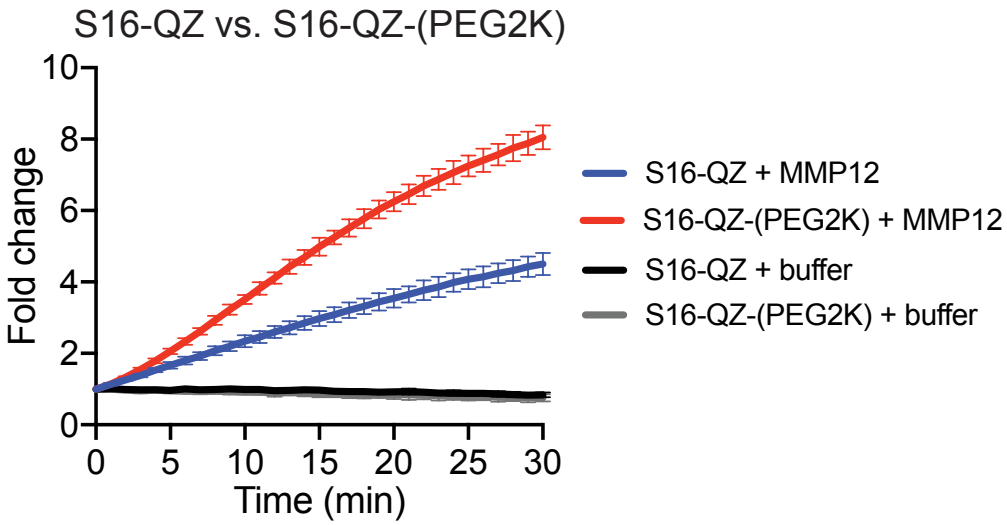


**Supplementary Figure S16. Cleavage of PEGylated imaging probe.** The quenched probe S16-QZ and the PEGylated version, S16-QZ-(PEG2K), were incubated with recombinant MMP12, and fluorescence activation was monitored over time ($n$ = 4 replicates; mean ± s.d.).

**Supplementary Table S1. Peptide sequences used throughout the study.**

| Name | Sequence | Readout (sample type) |
|---|---|---|
| S1-Q | (5FAM)-GGPQGIWGQ-K(CPQ2)-(PEG2)-C-NH2 | Fluorescence (in vitro / ex vivo) |
| S2-Q | (5FAM)-GGLVPRGSG-K(CPQ2)-(PEG2)-C-NH2 | Fluorescence (in vitro / ex vivo) |
| S3-Q | (5FAM)-GGPVGLIG-K(CPQ2)-(PEG2)-C-NH2 | Fluorescence (in vitro / ex vivo) |
| S4-Q | (5FAM)-GGPLGVRGK-K(CPQ2)-(PEG2)-C-NH2 | Fluorescence (in vitro / ex vivo) |
| S5-Q | (5FAM)-GRQRRALEKG-K(CPQ2)-(PEG2)-GC-NH2 | Fluorescence (in vitro / ex vivo) |
| S6-Q | (5FAM)-GGGSGRSANAKG-K(CPQ2)-(PEG2)-GC-NH2 | Fluorescence (in vitro / ex vivo) |
| S7-Q | (5FAM)-GKPISLISSG-K(CPQ2)-(PEG2)-GC-NH2 | Fluorescence (in vitro / ex vivo) |
| S8-Q | (5FAM)-GILSRIVGGG-K(CPQ2)-(PEG2)-GC-NH2 | Fluorescence (in vitro / ex vivo) |
| S9-Q | (5FAM)-GRPKPVE(Nval)WRKG-K(CPQ2)-(PEG2)-GC-NH2 | Fluorescence (in vitro / ex vivo) |
| S10-Q | (5FAM)-GIQQRSLGGG-K(CPQ2)-(PEG2)-GC-NH2 | Fluorescence (in vitro / ex vivo) |
| S11-Q | (5FAM)-GGVPRGG-K(CPQ2)-(PEG2)-GC-NH2 | Fluorescence (in vitro / ex vivo) |
| S12-Q | (5FAM)-GSGSKIIGGG-K(CPQ2)-(PEG2)-GC-NH2 | Fluorescence (in vitro / ex vivo) |
| S13-Q | (5FAM)-GAANLTRG-K(CPQ2)-(PEG2)-GC-NH2 | Fluorescence (in vitro / ex vivo) |
| S14-Q | (5FAM)-GLAQAPhe(homo)RSG-K(CPQ2)-(PEG2)-GC-NH2 | Fluorescence (in vitro / ex vivo) |
| S15-Q | (5FAM)-GSPLAQAVRSSG-K(CPQ2)-(PEG2)-GC-NH2 | Fluorescence (in vitro / ex vivo) |
| S16-Q | (5FAM)-GPVPLSLVMG-K(CPQ2)-(PEG2)-GC-NH2 | Fluorescence (in vitro / ex vivo) |
| S17-Q | (5FAM)-GSQPRIVGGG-K(CPQ2)-(PEG2)-GC-NH2 | Fluorescence (in vitro / ex vivo) |
| S19-Q | (5FAM)-GGLGPKGQTG-K(CPQ2)-(PEG2)-C-NH2 | Fluorescence (in vitro / ex vivo) |
| S20-Q | (5FAM)-GGQTCKCSCK-K(CPQ2)-(PEG2)-C-NH2 | Fluorescence (in vitro / ex vivo) |
| S1-M | e(+2G)(+6V)ndneeG(+10F)(+1F)s(+1A)r-ANP-GGPQGIWGQGC | LC-MS/MS (in vitro / ex vivo) |
| S2-M | eG(+6V)ndneeGF(+1F)s(+1A)r-ANP-GGLVPRGSGGC | LC-MS/MS (in vitro / ex vivo) |
| S3-M | e(+3G)(+1V)ndneeGFFs(+4A)r-ANP-GGPVGLIGGC | LC-MS/MS (in vitro / ex vivo) |
| S4-M | e(+2G)Vndnee(+2G)FFs(+4A)r-ANP-GGPLGVRGKGC | LC-MS/MS (in vitro / ex vivo) |
| S5-M | e(+3G)(+1V)ndneeG(+10F)FsAr-ANP-GRQRRALEKGC | LC-MS/MS (in vitro / ex vivo) |
| S6-M | e(+2G)Vndnee(+2G)F(+10F)sAr-ANP-GGGSGRSANAKGC | LC-MS/MS (in vitro / ex vivo) |
| S7-M | e(+2G)(+6V)ndneeGFFsAr-ANP-GKPISLISSGC | LC-MS/MS (in vitro / ex vivo) |
| S8-M | eGVndneeGF(+10F)s(+4A)r-ANP-GILSRIVGGGC | LC-MS/MS (in vitro / ex vivo) |
| S9-M | eG(+6V)ndneeG(+10F)Fs(+4A)r-ANP-GRPKPVE(Nval)WRKGC | LC-MS/MS (in vitro / ex vivo) |
| S10-M | e(+3G)(+1V)ndnee(+2G)(+10F)Fs(+4A)r-ANP-GIQQRSLGGGC | LC-MS/MS (in vitro / ex vivo) |
| S11-M | e(+2G)Vndnee(+3G)(+10F)(+1F)s(+4A)r-ANP-GGVPRGGC | LC-MS/MS (in vitro / ex vivo) |
| S12-M | eGVndneeG(+10F)(+10F)sAr-ANP-GSGSKIIGGGC | LC-MS/MS (in vitro / ex vivo) |
| S13-M | e(+2G)(+6V)ndnee(+3G)(+10F)(+1F)s(+4A)r-ANP-GAANLTRGC | LC-MS/MS (in vitro / ex vivo) |
| S14-M | eG(+6V)ndneeG(+10F)(+10F)sAr-ANP-GLAQAPhe(homo)RSGC | LC-MS/MS (in vitro / ex vivo) |
| S15-M | e(+3G)(+1V)ndnee(+2G)(+10F)(+10F)sAr-ANP-GSPLAQAVRSSGC | LC-MS/MS (in vitro / ex vivo) |
| S16-M | e(+2G)VndneeG(+10F)(+10F)s(+4A)r-ANP-GPVPLSLVMGC | LC-MS/MS (in vitro / ex vivo) |
| S17-M | eGVndnee(+2G)(+10F)(+10F)s(+4A)r-ANP-GSQPRIVGGGC | LC-MS/MS (in vitro / ex vivo) |
| S19-M | e(+2G)(+6V)ndnee(+3G)(+1F)(+1F)s(+1A)r-ANP-GGLGPKGQTGGC | LC-MS/MS (in vitro / ex vivo) |
| S20-M | eG(+6V)ndnee(+3G)(+1F)Fs(+4A)r-ANP-GGQTCKCSCKGC | LC-MS/MS (in vitro / ex vivo) |

| | | |
|---|---|---|
| S1-Z | U-eeeeeeee-X-GGPQGIWGQG-rrrrrrrrr-X-K(Cy3)-NH2 | Fluorescence (in situ) |
| S2-Z | U-eeeeeeee-X-GGLVPRGSGG-rrrrrrrrr-X-K(Cy5)-NH2 | Fluorescence (in situ) |
| S3-Z | U-eeeeeeee-X-GGPVGLIGG-rrrrrrrrr-X-K(5FAM)-NH2 | Fluorescence (in situ) |
| S4-Z | U-eeeeeeee-X-GPLGVRGKG-rrrrrrrrr-X-K(5FAM)-NH2 | Fluorescence (in situ) |
| S5-Z | U-eeeeeeee-X-GRQRRALEKG-rrrrrrrrr-X-K(Cy3)-NH2 | Fluorescence (in situ) |
| S6-Z | U-eeeeeeee-X-GSGRSANAG-rrrrrrrrr-X-K(Cy5)-NH2 | Fluorescence (in situ) |
| S7-Z | U-eeeeeeee-X-GKPISLISSG-rrrrrrrrr-X-K(5FAM)-NH2 | Fluorescence (in situ) |
| S8-Z | U-eeeeeeee-X-GILSRIVGGG-rrrrrrrrr-X-K(5FAM)-NH2 | Fluorescence (in situ) |
| S9-Z | U-eeeeeeee-X-GRPKPVE(Nval)WRKG-rrrrrrrrr-X-K(5FAM)-NH2 | Fluorescence (in situ) |
| S10-Z | U-eeeeeeee-X-GIQQRSLGGG-rrrrrrrrr-X-K(5FAM)-NH2 | Fluorescence (in situ) |
| S11-Z | U-eeeeeeee-X-GGGVPRGGG-rrrrrrrrr-X-K(5FAM)-NH2 | Fluorescence (in situ) |
| S12-Z | U-eeeeeeee-X-GSGSKIIGGG-rrrrrrrrr-X-K(Cy3)-NH2 | Fluorescence (in situ) |
| S13-Z | U-eeeeeeee-X-GGAANLTRGG-rrrrrrrrr-X-K(Cy3)-NH2 | Fluorescence (in situ) |
| S14-Z | U-eeeeeeee-X-GLAQAPhe(homo)RSG-rrrrrrrrr-X-K(Cy3)-NH2 | Fluorescence (in situ) |
| S15-Z | U-eeeeeeee-X-GSPLAQAVRSSG-rrrrrrrrr-X-K(Cy3)-NH2 | Fluorescence (in situ) |
| S16-Z | U-eeeeeeee-X-GPVPLSLVMG-rrrrrrrrr-X-K(5FAM)-NH2 | Fluorescence (in situ) |
| S17-Z | U-eeeeeeee-X-GSQPRIVGGG-rrrrrrrrr-X-K(Cy5)-NH2 | Fluorescence (in situ) |
| S18-Z | U-eeeeeeee-X-GGGHARLVHVG-rrrrrrrrr-X-K(Cy3)-NH2 | Fluorescence (in situ) |
| S19-Z | U-eeeeeeee-X-GGLGPKGQTGG-rrrrrrrrr-X-K(Cy3)-NH2 | Fluorescence (in situ) |
| S20-Z | U-eeeeeeee-X-GGQTCKCSCKG-rrrrrrrrr-X-K(Cy5)-NH2 | Fluorescence (in situ) |
| dS6-Z | U-eeeeeeee-X-GsGrsanaG-rrrrrrrrr-X-K(Cy5)-NH2 | Fluorescence (in situ) |
| S6-QZ | (QSY21)-eeeeeeeee-c-o-GSGRSANAG-rrrrrrrrr-K(Cy5)-NH2 | Fluorescence (in situ) |
| dS6-QZ | (QSY21)-eeeeeeeee-c-o-GsGrsanaG-rrrrrrrrr-K(Cy5)-NH2 | Fluorescence (in situ) |
| dS16-Z | U-eeeeeeee-X-GpvplslvmG-rrrrrrrrr-X-K(5FAM)-NH2 | Fluorescence (in situ) |
| S16-QZ | (QSY21)-eeeeeeeee-c-o-GPVPLSLVMG-rrrrrrrrr-K(Cy5)-NH2 | Fluorescence (in situ / in vivo) |
| dS16-QZ | (QSY21)-eeeeeeeee-c-o-GpvplslvmG-rrrrrrrrr-K(Cy5)-NH2 | Fluorescence (in situ / in vivo) |
| S16 | GPVPLSLVMG | Cleavage motif |
| polyR | rrrrrrrrr-X-K(Cy7)-NH2 | Fluorescence (in situ) |

*Notes:*

Lower case: *d*-stereoisomer.

Nomenclature: Q = quenched, M = mass barcoded, Z = zymography

NH2: amidated C-terminus

5FAM-CPQ2: FRET pair, with 5-Carboxyfluorescein as fluorophore and CPQ2 as quencher

QSY21-Cy5: FRET pair, with Cy5 as fluorophore and QSY21 as quencher

PEG2: diethylene-glycol

ANP: 3-Amino-3-(2-nitrophenyl)propionic acid

o: 5-amino-3-oxopentanoyl

U: succinoyl

X: 6-aminohexanoyl

Phe(homo): homo-phenylalanine

Nval: Norvaline

**Supplementary Table S2. Buffer solutions used throughout the study.**

| Buffer name / description | Recipe |
|---|---|
| Bead wash buffer | 0.5% (w/v) bovine serum albumin (BSA), 0.01% (v/v) Tween-20 in PBS |
| S6-Z assay buffer | 50 mM Tris, 0.01% (v/v) Tween 20, 1% (w/v) BSA, pH 7.4 |
| S2-Z, S10-Z / serine protease assay buffer | 50 mM Tris, 150 mM NaCl, 10 mM $CaCl_2$, 0.05% (v/v) Brij-35, 1% (w/v) BSA, pH 7.5 |
| S16-Z / MMP assay buffer | 50 mM Tris, 300 mM NaCl, 10 mM $CaCl_2$, 2 μM $ZnCl_2$, 0.02% (v/v) Brij-35, 1% (w/v) BSA, pH 7.5 |

**Supplementary Table S3. Protease / AZP pairs for library characterization.**

| Protease | AZP(s) |
|---|---|
| MMP13 (Enzo Life Sciences) | S1-Z, S3-Z, S7-Z, S14-Z, S15-Z, S16-Z, and S19-Z |
| PRSS3 (R&D Systems) | S2-Z, S6-Z, S9-Z, S11-Z, S12-Z, S13-Z, S17-Z, and S20-Z |
| KLK14 (R&D Systems) | S5-Z, S8-Z, and S18-Z |
| KLK2 (R&D Systems) | S10-Z |

**Supplementary Table S4. Strategies for profiling protease activity *ex vivo*.**

| Assay type | Sample type | Throughput | Spatial information | Applications |
|---|---|---|---|---|
| Cleavage of fluorogenic substrates | Recombinant enzymes, tissue homogenates, biofluids | Single probe per reaction volume. | No; bulk assay | Measure substrate cleavage kinetics in real time |
| Pooled screen with barcoded substrates | Recombinant enzymes, tissue homogenates, biofluids | Many probes per reaction volume. | No; bulk assay | Identify lead probes from substrate library |
| *In situ* localization with AZPs | Fresh-frozen tissue sections | Small numbers of probes per tissue | Yes | Characterize lead probes across tissue sections<br><br>Study protease biology |

**References**

1. Ellwood-Yen, K. *et al.* Myc-driven murine prostate cancer shares molecular features with human prostate tumors. *Cancer Cell* **4**, 223–238 (2003).